

Electronic Supplementary Information

Computational Investigation of Acetylene Hydrogenation to Ethylene over Transition Metal–Exchanged Chabazite Zeolites: Mechanistic Insights and Descriptor-Based Predictions

Thana Maihom^{a,b*}, Michael Probst^c, Jumras Limtrakul^d

^aDivision of Chemistry, Department of Physical and Material Sciences, Faculty of Liberal Arts and Science, Kasetsart University, Kamphaeng Saen Campus, Nakhon Pathom 73140, Thailand.

^bCenter for Advanced Studies in Nanotechnology for Chemical, Food and Agricultural Industries, Kasetsart University Institute for Advanced Studies, Kasetsart University, Bangkok, 10900, Thailand.

^cInstitute of Ion Physics and Applied Physics, University of Innsbruck, Innsbruck 6020, Austria.

^dSchool of Energy Science and Engineering, Vidyasirimedhi Institute of Science and Technology, Rayong 2120, Thailand.

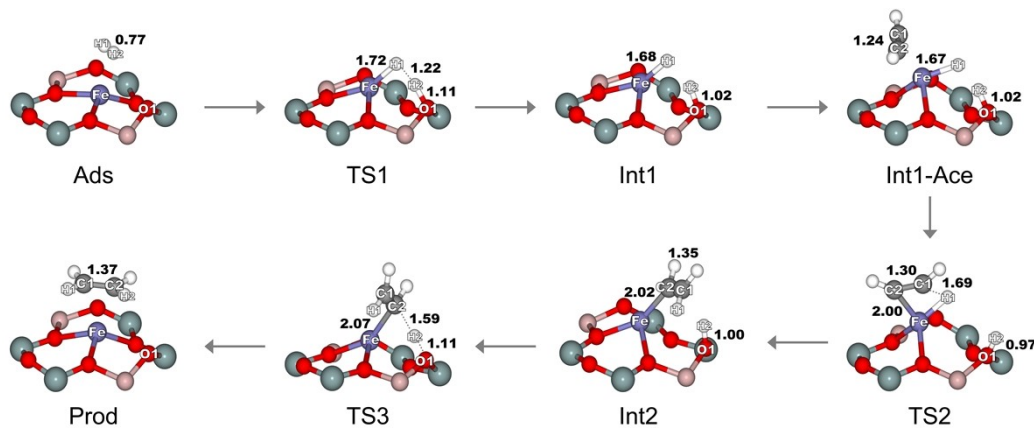


Fig. S1. Optimized structures for the acetylene hydrogenation to ethylene on Fe-CHA.

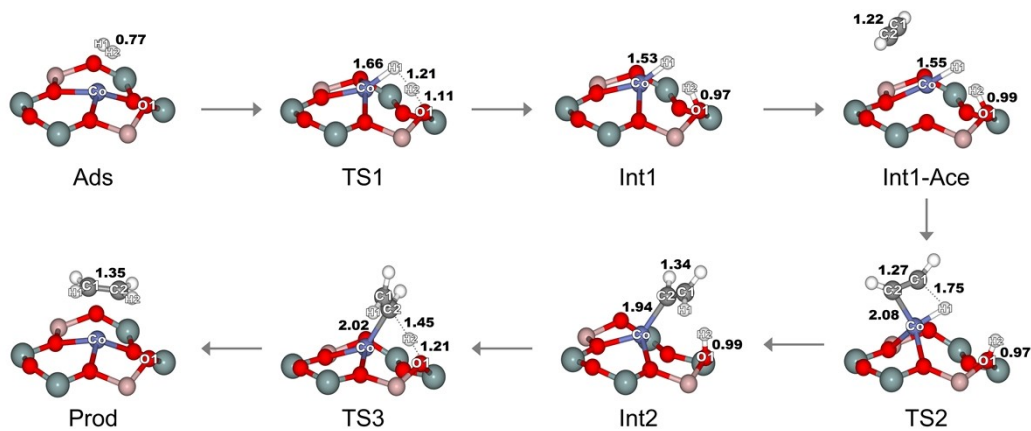


Fig. S2. Optimized structures for the acetylene hydrogenation to ethylene on Co-CHA.

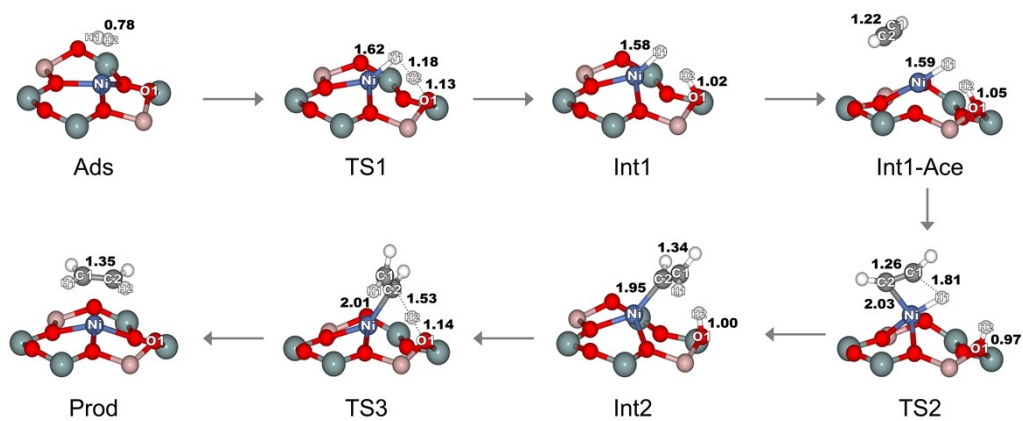


Fig. S3. Optimized structures for the acetylene hydrogenation to ethylene on Ni-CHA.

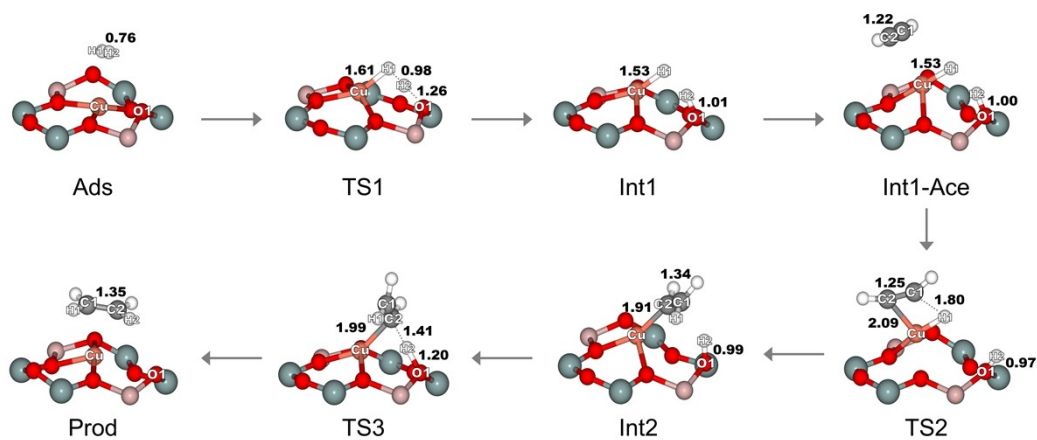


Fig. S4. Optimized structures for the acetylene hydrogenation to ethylene on Cu-CHA.

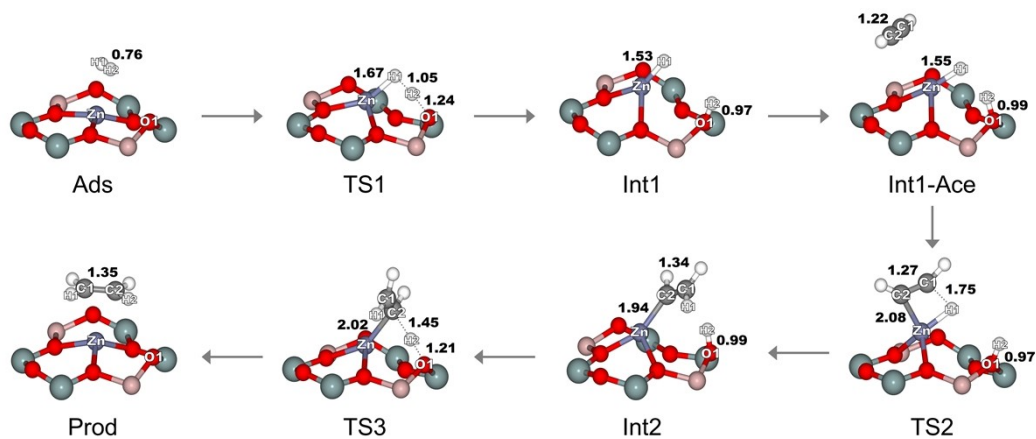


Fig. S5. Optimized structures for the acetylene hydrogenation to ethylene on Zn-CHA.

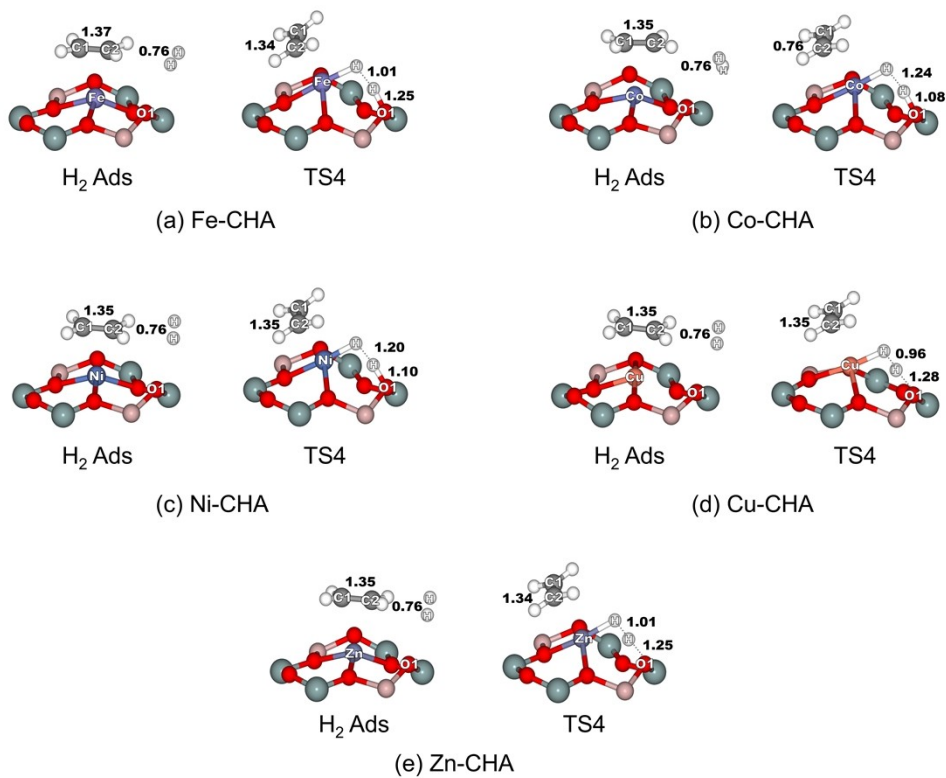


Fig. S6. Optimized structures of H_2 dissociation in the presence of adsorbed ethylene on (a) Fe-CHA, (b) Co-CHA, (c) Ni-CHA, (d) Cu-CHA and (e) Zn-CHA.

Table S1. Atomic partial charges from NBO analysis for key intermediates and transition states of M-CHA catalysts.

Zeolite	Hydride charge in TS1 (e)	Metal charge in Int1-Ace (e)	Metal charge in TS3 (e)	Ethenyl total charge in TS2 (e)
Fe-CHA	-0.330	0.919	-1.227	-0.246
Co-CHA	-0.326	1.022	-1.233	-0.171
Ni-CHA	-0.264	0.919	-1.231	-0.207
Cu-CHA	-0.157	0.836	-1.247	-0.026
Zn-CHA	-0.290	1.099	-1.244	-0.246

Table S2. Overall activation free energies ($\Delta G^{\#}_{\text{overall}}$) calculated using the M06-L functional and compared with M06-L-D3, B3LYP-D3 and B3LYP-D3(BJ) results obtained from single point energy calculations on M06-L optimized structures.

Zeolite	M06-L	M06-L-D3	B3LYP-D3	B3LYP-D3(BJ)
Fe-CHA	29.7	28.0	33.3	33.4
Co-CHA	32.7	31.0	32.7	34.0
Ni-CHA	21.8	20.2	20.5	20.6
Cu-CHA	16.0	14.4	15.8	15.5
Zn-CHA	37.9	36.1	35.2	35.3

Table S3. Overall activation free energies ($\Delta G^{\#}_{\text{overall}}$) calculated using the def2-SVP basis set and compared with def2-TZVP results obtained from single-point energy calculations on def2-SVP-optimized structures, with thermal corrections derived from def2-SVP.

Zeolite	def2-SVP	def2-TZVP
Fe-CHA	29.7	31.7
Co-CHA	32.7	32.9
Ni-CHA	21.8	23.2
Cu-CHA	16.0	16.5
Zn-CHA	37.9	40.4

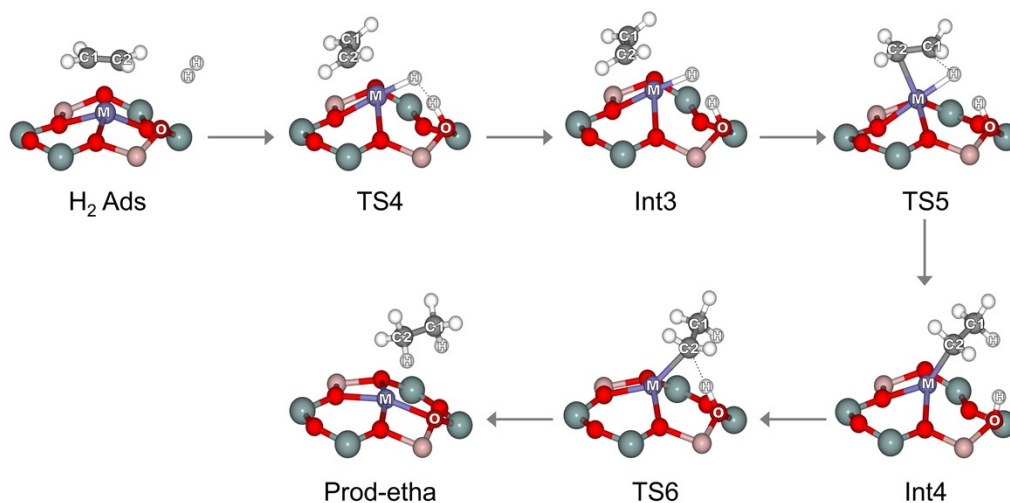


Fig. S7. Reaction mechanism for the over-hydrogenation of ethylene to ethane on Fe-CHA. Si, Al, O, C, H and metal atoms are represented in green, pink, red, gray, white, and blue, respectively.

Table S4. Relative Gibbs free energies for the over-hydrogenation of ethylene to ethane on M-CHA.

Species	Relative Gibbs free energy (kcal/mol)				
	Fe-CHA	Co-CHA	Ni-CHA	Cu-CHA	Zn-CHA
H ₂ Ads	-30.7	-39.1	-41.4	-31.1	-36.6
TS4	-5.4	-12.8	-22.0	-20.9	-17.3
Int3	-5.5	-12.4	-20.9	-22.6	-20.7
TS5	14.4	4.2	-10.4	-15.0	14.1
Int4	-22.2	-27.5	-36.4	-42.6	-41.1
TS6	-17.5	-26.3	-31.2	-35.5	-32.3
Prod-etha	-60.9	-65.6	-71.7	-67.4	-64.4
$\Delta G^{\#}_{\text{overall}}$	45.1	43.3	31.0	16.1	50.7

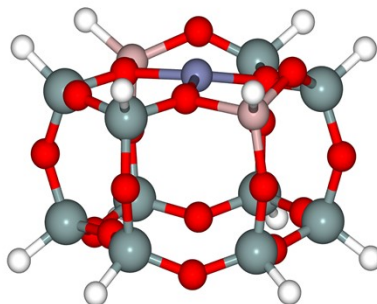


Fig. S8. 12T cluster model of M-CHA. Si, Al, O, H and metal atoms are represented in green, pink, red, white, and blue, respectively.

Table S5. Relative energies of the systems along the reaction coordinate with 42T and 12T cluster models.

Species	Relative Gibbs free energy (kcal/mol)									
	Fe-CHA		Co-CHA		Ni-CHA		Cu-CHA		Zn-CHA	
	42T	12T	42T	12T	42T	12T	42T	12T	42T	12T
Ads	10.4	13.3	3.2	2.0	3.3	5.3	6.7	5.7	5.1	5.5
TS1	32.7	39.0	24.6	25.9	17.7	20.1	18.7	19.0	21.0	25.6
Int1	33.1	39.7	25.0	25.9	18.1	20.8	16.6	21.2	13.2	20.4
Int1-Ace	30.3	46.0	23.4	30.7	14.8	25.2	13.4	28.2	16.9	29.7
TS2	40.1	54.5	35.9	46.9	25.0	38.6	22.7	38.6	43.0	57.7
Int2	-3.0	6.8	-11.0	-5.2	-16.7	-9.8	-20.1	-8.1	-19.1	-13.2
TS3	-1.5	9.2	-7.8	-6.1	-13.5	-8.0	-14.6	-6.9	-13.5	-7.2
Prod	-42.4	-32.6	-49.1	-42.7	-49.6	-44.1	-39.6	-34.6	-46.3	-38.5
$\Delta G^{\#}_{\text{overall}}$	29.7	41.2	32.7	44.9	21.7	33.3	16.0	32.9	37.9	52.2

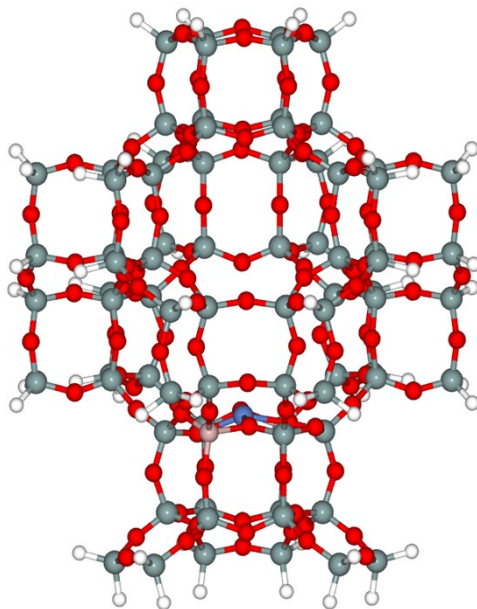


Fig. S9. 78T cluster model of M-CHA. Si, Al, O, C, H and metal atoms are represented in green, pink, red, gray, white, and blue, respectively.

Table S6 Overall activation free energies ($\Delta G^{\#}_{\text{overall}}$) calculated using the 72T cluster model, obtained from single-point energy calculations on 42T cluster-optimized structures, with thermal corrections derived from the 42T cluster.

Zeolite	42T	72T
Fe-CHA	29.7	26.3
Co-CHA	32.7	32.3
Ni-CHA	21.8	20.5
Cu-CHA	16.0	15.1
Zn-CHA	37.9	37.0

Table S7. R^2 and RMSEs values for the correlation between one descriptor and the overall activation barrier ($\Delta G^{\#}_{\text{overall}}$).

Descriptors	R^2	RMSE
B_{M-O}	0.002	10.0
Di	0.718	5.3
E_H	0.071	9.7
E_L	0.195	9.0
μ	0.317	8.3
η	0.086	9.6
ω	0.207	8.9
ρ	0.817	4.3